*Thoracic Cancer*

WILEY

ORIGINAL ARTICLE OPEN ACCESS

# Exosomal PVRL4 Promotes Lung Adenocarcinoma Progression by Enhancing the Generation of Myeloid-Derived Suppressor Cell-Secreted TGF-β1

Yahai Liang[1] | Jinmei Li[1] | Lihua Zhang[1] | Jinling Zhou[2] | Meilian Liu[1] | Xiaoxia Peng[1] | Weizhen Zheng[1] | Zhennan Lai[1]

[1]Department of Pulmonary Oncology, Affiliated Hospital of Guangdong Medical University, Zhanjiang, China | [2]Anesthesia Surgery Center, Affiliated Hospital of Guangdong Medical University, Zhanjiang, China

**Correspondence:** Zhennan Lai (laizhenn@163.com)

**Received:** 20 August 2024 | **Revised:** 25 October 2024 | **Accepted:** 11 November 2024

**Funding:** The authors received no specific funding for this work.

**Keywords:** exosome | immunosuppressive activity | LUAD | MDSCs | PBMCs | PVRL4 | TGF-β1

## ABSTRACT

**Background:** The cancer cell marker poliovirus receptor-like protein 4 (PVRL4) has been shown to be highly expressed in many cancers, including lung cancer. Myeloid-derived suppressor cells (MDSCs) are a population of immature myeloid cells with immunosuppressive roles that can attenuate the anticancer response. Here, the precise functions and the relationship between PVRL4 and MDSCs in lung adenocarcinoma (LUAD) progression were investigated.

**Methods:** Detection of levels of mRNAs and proteins was conducted using qRT-PCR and western blotting. The CCK-8, colony formation, transwell, wound healing assays, and flow cytometry were used to explore cell growth, invasion, migration, and apoptosis, respectively. ELISA analysis detected TGF-β1 contents. LUAD mouse models were established for in vivo assay. Exosomes were isolated by ultracentrifugation. MDSCs were induced from peripheral blood mononuclear cells (PBMCs) by cytokine or co-culture with cancer cells.

**Results:** LUAD tissues and cells showed high PVRL4 expression, and PVRL4 deficiency suppressed LUAD cell proliferation, invasion, migration, and induced cell apoptosis in vitro, and impeded LUAD growth in vivo. Thereafter, we found that PVRL4 was packaged into exosomes in LUAD cells, and could be transferred into PBMCs to promote MDSC induction and the expression of MDSC-secreted TGF-β1. Functionally, the silencing of exosomal PVRL4 impaired LUAD cell proliferation, invasion, migration, and evoked cell apoptosis, which could be reversed by the incubation of TGF-β1-overexpressed MDSCs.

**Conclusion:** Exosomal PVRL4 promoted LUAD progression by inducing the secretion of TGF-β1 in MDSCs, indicating a novel direction for LUAD immunotherapy.

## 1 | Introduction

Lung adenocarcinoma (LUAD) is one of the deadliest cancers accounting for about 40% of all lung cancer cases [1, 2]. The majority of LUAD are incurable or advanced, so the 5-year survival of LUAD patients is only 15% [3, 4]. Surgery remains the standard therapy yet; however, there is a high risk of relapse [5]. Thus, a better understanding of the pathogenesis of LUAD is indispensable for developing effective therapeutic strategies for this disease.

In recent years, molecular targeted therapy using therapeutic monoclonal antibodies or small molecule agents to impact signal transduction has been recognized to play a fundamental role in precision medicine for oncotherapy [6, 7]. The achievement of anticancer effects of molecular targeted therapy is involved in

diverse mechanisms, including the suppression of cell angiogenesis, growth, and metastasis, the promotion of cell apoptosis, the enhancement antitumor immunity by promoting the cytotoxicity in T cells, decreasing immunosuppressive myeloid cells or triggering immunogenic cell death [8, 9]. Relative to conventional chemotherapy, targeted therapeutic drugs have fewer side effects and great advantages in efficacy and safety, and many of small-molecule targeted agents have been used clinically for the therapy of various cancers since the initial approval of the first tyrosine kinase inhibitor imatinib by the US FDA in 2001 [10–12]. In lung cancer, molecular alterations is also reported to be implicated in the progression of this cancer, and numerous of targeted antitumor drugs have been approved for lung cancer treatment or are being developed [13]. Poliovirus receptor-like protein 4 (PVRL4, or nectin-4) is an embryonic protein belonging to the PVRLs family that are adhesion receptors of the immunoglobulin superfamily [14]. It is a cancer cell marker that is highly expressed in many tumors of breast, ovarian, colon, lung, etc. [15–18] PVRL4 is implicated in modulating a variety of facets of cancer like metastasis, angiogenesis, proliferation, cancer relapse, drug resistance, etc., and is recognized as a promising molecule for targeted therapy in cancers [18]. Moreover, Tamura et al. showed that PVRL4 expression was elevated in canine primary lung adenocarcinoma, and was positively associated with tumor growth [19]. In addition, we found an increased expression of PVRL4 in LUAD tissues according to the Ualcan, Gepia, and Timer databases, indicating that PVRL4 deregulation may be related to LUAD progression. However, the precise functions of PVRL4 on LUAD tumorigenesis remain unclear.

Herein, this study investigated the action of PVRL4 on LUAC cell oncogenic phenotypes and tumor growth, and its protein mechanisms, which may provide a new direct for the development of molecular targeted therapy in LUAD.

## 2 | Materials and Methods

### 2.1 | Clinical Samples

Tumor tissues and adjacent normal tissues were collected from 31 newly diagnosed LUAD patients by surgery. None of them received the preoperative therapy. In addition, 5 mL venous blood was collected from healthy volunteers for human peripheral blood mononuclear cells (PBMCs) isolation. All the samples were stored at −80°C. This study was authorized by the institutional ethics committee of the Affiliated Hospital of Guangdong Medical University based on the Declaration of Helsinki.

### 2.2 | Cell Culture

LUAD cell lines A549 and HCC827 and the normal 16HBE cells were purchased from Procell (Wuhan, China) and then cultured in RPMI-1640 medium (PM150110) plus1% penicillin/streptomycin (PB180120) and 10% FBS (164210-50) (Procell) at 37°C with 5% $CO_2$.

### 2.3 | qRT-PCR

Total RNAs were isolated using the TRIzol (Pufei, Shanghai, China), and then reversed transcribed into cDNAs following the recommended protocol of PrimerScript RT Reagent Kit (TaKaRa, Kyoto, Japan). Next, qRT-PCR was conducted using cDNA templates and SYBR Green Taq Mix (Takara). The fold change was determined using the $2^{-\Delta\Delta Ct}$ method normalizing to β-actin expression. Table 1 lists the primers for qRT-PCR.

### 2.4 | Western Blotting

Total proteins were isolated by incubating cells or tissues with 500 μL RIPA lysis buffer (Beyotime, Beijing, China). Then the lysates were separated by PAGE with a 4%–20% gradient Tris-glycine gel, and subsequently transferred from the gel to a nitrocellulose membrane at 30 V for 1 h. After being blocked in 5% milk for 1 h, the PVRL4 (ab155692, 1:2000), Alix (ab275377, 1:1000), CD63 (ab271286, 1:1000), TGF-β1 (ab215715, 1:1000) and β-actin (ab8226, 1:2000) primary antibodies were used to incubate overnight at 4°Cwith the membranes, which were then incubated with matched HRP-conjugated secondary antibodies at 37°Cfor 2 h. The band densities were determined by using an ECL kit (Beyotime).

### 2.5 | Cell Transfection

The short hairpin RNA (shRNA) was designed to target PVRL4 (sh-PVRL4) with scramble shRNA as the control (sh-NC). Then sh-PVRL4 or sh-NC was cloned into the lentiviral plasmids (ATCC, Rockville, MD, USA) and then incubated with 293T cells. Forty-eight hours later, lentiviral particles carrying sh-NC or sh-PVRL4 were obtained by ultracentrifugation from 293T cell supernatants. For overexpression of TGF-β1, the CDS region of TGF-β1 encoding the full-length protein was subcloned into pcDNA3.1 plasmids at *BamH1* and *EcoR1* sites (GenePharma, Shanghai, China), termed TGF-β1, and the scramble plasmid served as the control (pcDNA). The recombinant lentiviral particles or plasmids were transfected into LUAD cells or MDSCs using the Lipofectamine 3000 (Invitrogen, Carlsbad, CA, USA) according to the instruction manuals.

### 2.6 | Exosome Isolation and Identification

The culture medium of A549 and HCC827 cells that were transfected with or without sh-PVRL4 or sh-NC were harvested and centrifuged at 300 g for 10 min to obtain cell supernatant. Then, the cell supernatant was centrifuged at 10000 g for 20 min and at 100000 × g for 70 min, successively. The precipitates were then resuspended in 1 × PBS, filtered with 0.22 μm strainer, and then centrifuged at 100000 × g for 1 h. Then exosome pellets were

**TABLE 1** | The primers for qRT-PCR.

| Name | Primers for qRT-PCR (5′-3′) | |
|---|---|---|
| PVRL4 | Forward | TGTCCTGGTCCCAGATATGAGT |
| | Reverse | CCGTAGGGTCCCATTCTCCT |
| β-Actin | Forward | CTTCGCGGGCGACGAT |
| | Reverse | CCACATAGGAATCCTTCTGACC |

collected, named HCC827-Exo, A549-Exo, HCC827-Exo$^{sh-NC}$, A549-Exo$^{sh-NC}$, HCC827-Exo$^{sh-PVRL4}$, or A549-Exo$^{sh-PVRL4}$, and resuspended in PBS for subsequent analysis. The morphology of exosomes was observed by a transmission electron microscope (TEM) (JEM-1010, JEOL, Tokyo, Japan). In addition, resuspended exosomes were lysed on ice, and protein levels of exosomal markers (Alix, CD63, and CD9) were examined using western blotting.

### 2.7 | Human MDSC Induction

Human PBMCs were isolated from the blood samples of Healthy donors using the Lymphocyte separation medium (TBD, Beijing, China) as per the manufacturer's protocol. To generate MDSCs, PBMCs (1×106 cells/mL) were incubated with 10 ng/mL GM-CSF, 10 ng/mL IL-6, and 10% heat-inactivated FBS in RPMI-1640 medium for 1 week. The medium was replaced by fresh medium for 3 days. In addition, PBMCs were cultured in RPMI-1640 medium containing 10% exosome-depleted FBS at a density of 2×10 [5], and then incubated with 10 μg/mL exosomes (HCC827-Exo, A549-Exo, HCC827-Exo$^{sh-NC}$, A549-Exo$^{sh-NC}$, HCC827-Exo$^{sh-PVRL4}$, or A549-Exo$^{sh-PVRL4}$) for 48 h. Then, the percentage of CD14$^{+}$HLA-DR$^{-}$ MDSCs was determined using flow cytometry.

### 2.8 | Cellular Uptake of Exosomes

Exosomes were resuspended in 50 μL PBS and then mixed with 1 mL of Diluent C. Thereafter, 4 μL PKH67 dye diluted in 1 mL of diluent C was added to incubate with exosomes for 15 min. Then the exosome mixture was incubated with 3 mL 0.5% BSA to remove unincorporated dye contamination. After centrifugation at 100000×g for 70 min, purified PKH67 exosomes were collected and incubated with PBMCs for 48 h. Cells were stained with DAPI at the end of incubation to observe nuclei. The exosomes uptake was observed using a fluorescence microscope.

### 2.9 | Cell Counting Kit-8 (CCK-8) Assay

Assigned A549 and HCC827 cells were placed onto a quantity of 1×104 cells/well in a 96-well plate, and then incubated with 15 μL CCK-8 solution for 24, 48 or 72 h. Finally, the absorbance was tested at 450 nm.

### 2.10 | Colony Formation Assay

Assigned A549 and HCC827 cells were grown at 37°C for 10–14 days. After washing with PBS, cells were fixed in methanol for 15 min and then labeled with crystal violet (0.1%) for 30 min. Colonies ($\geq$50 cells) were observed and counted.

### 2.11 | Transwell Assay

Transwell Chamber inserts pre-coated with Matrigel (BD Biosciences, Franklin Lakes, NJ, USA) were used for cell invasion analysis. After the indicated treatment, A549 and HCC827 cells were plated into the upper chambers of Transwell plates containing serum-free RPMI-1640 medium. Six hundred microliters of medium supplemented with 10% FBS was plated into the lower chambers. Twenty-four hours later, the invaded cells were fixed with 4% formalin and stained with crystal violet. The stained cells were then visualized and counted.

### 2.12 | Wound Healing Assay

After the indicated treatment, A549 and HCC827 cells were seeded at 1×105 cells/well in a 6-well plate with serum-free medium. Then, the cell monolayer was scraped using a 1-ml pipette tip and washed 3 times with PBS (time 0). Next, a complete growth medium was used to culture the cell for another 24 h. Images were captured using a light microscope at 0 and 24 h, and the wound closure was recorded to assess cell migration.

### 2.13 | Flow Cytometry

For cell apoptosis analysis, A549 and HCC827 cells with indicated treatment were resuspended in 1× Annexin V binding buffer containing 10 μL Annexin V-FITC and 10 μL propidium iodide (PI) (BD Biosciences), and incubated for 15 min avoiding light. The apoptotic cells were analyzed by flow cytometer (BD Biosciences).

To measure the population of CD14$^{+}$HLA-DR$^{-}$ MDSCs, PBMCs incubated with assigned exosomes were stained with anti-human CD14-FITC and anti-human HLA-DR-PE (BD Biosciences) at 37°C for 30 min. Lastly, a flow cytometric analysis was performed.

### 2.14 | ELISA Analysis

The supernatant of assigned A549 and HCC827 cells was collected by centrifugalization and the concentrations of TGF-β1 were determined using the ELISA Kits (Abcam) in line with the manufacturers' instructions.

### 2.15 | In Vivo Assay

A549 cells were infected with sh-NC or sh-PVRL4 lentiviral particles and 8 μg/mL polybrene. Then stable infected cells (4×10 [6]/0.2 mL PBS) were subcutaneously inoculated into BALB/c mice (4–5 weeks old, $n = 12$, Slaike Jingda Laboratory, Hunan, China). The tumor volume was monitored every 5 days. At day 25, mice were killed and tumors were isolated and weighed.

### 2.16 | Immunohistochemistry (IHC) Staining

The human LUAD tissues or mouse xenograft tissues were fixed with 10% formaldehyde and then embedded in paraffin. Paraffin-embedded tissues were cut into 4-μm sections and

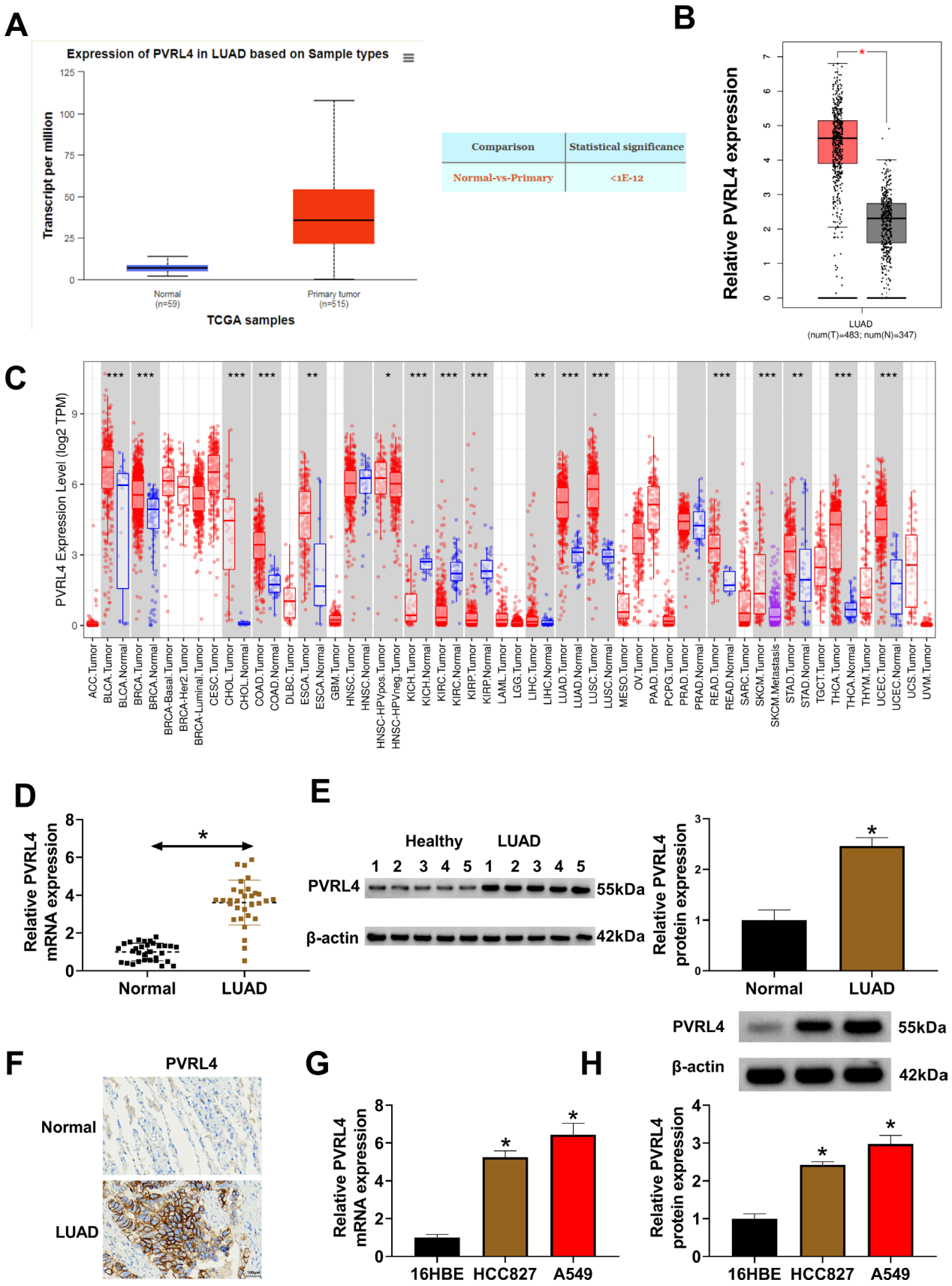


**FIGURE 1** | PVRL4 is highly expressed in LUAD tissues and cells. (A–C) The Ualcan, Gepia, and Timer databases indicated that PVRL4 was highly expressed in LUAD tissues. (D–F) qRT-PCR, western blotting, and IHC analysis showed the expression profiles of PVRL4 in clinical LUAD tissues and normal tissues. (G, H) qRT-PCR and western blotting for the expression profiles of PVRL4 in LUAD cell lines and normal 16HBE cells. *$p < 0.05$.

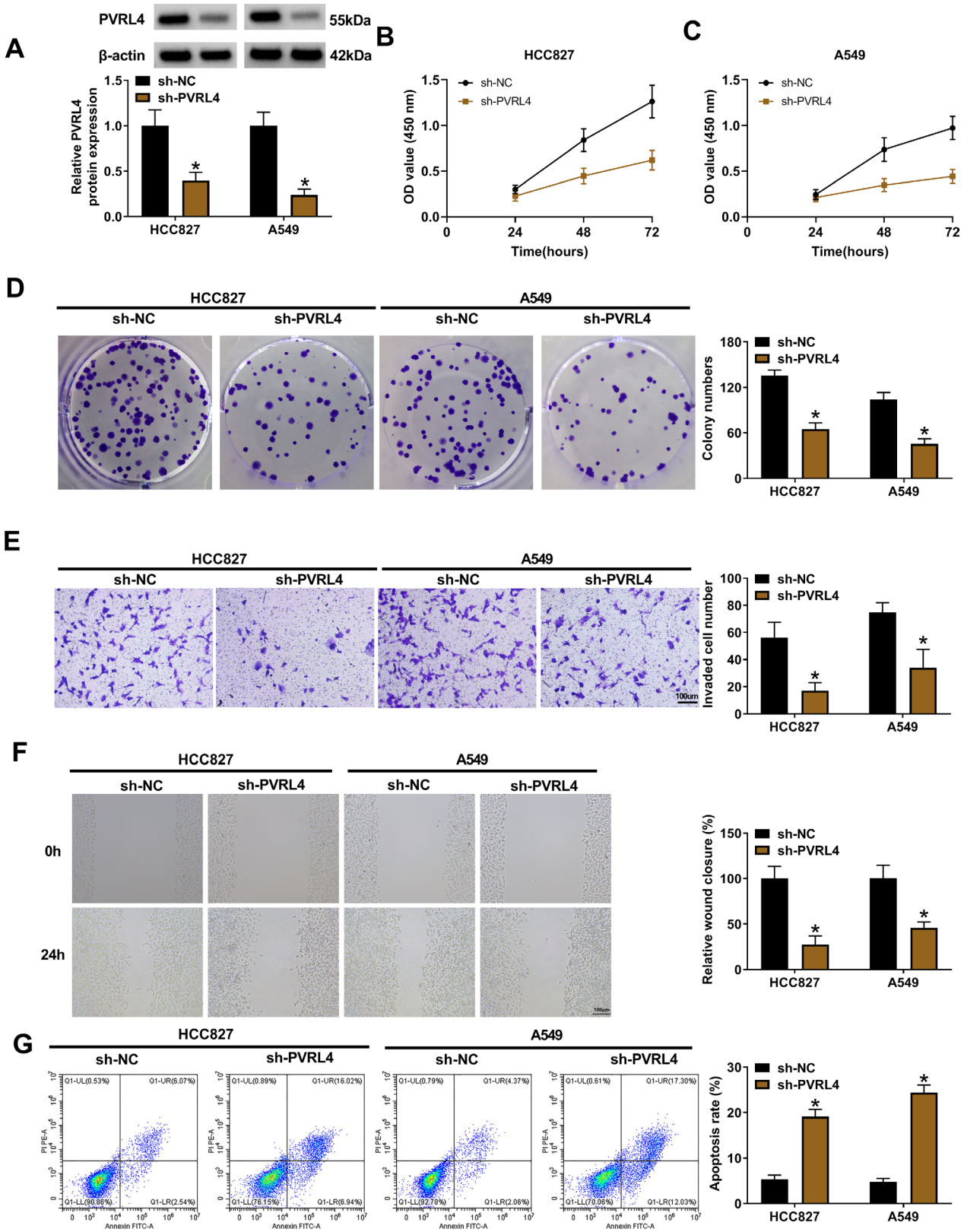


**FIGURE 2** | PVRL4 silencing suppresses LUAD cell proliferation, invasion, and migration and induces cell apoptosis. (A-G) The sh-PVRL4 or sh-NC was transfected into A549 and HCC827 cells. (A) Western blotting for PVRL4 levels in cells. (B-D) CCK-8 and colony formation assays for cell proliferation. (E) Transwell for cell invasion. (F) Wound healing assay for cell migration. (G) Flow cytometry analysis for cell apoptosis. *$p < 0.05$.

then subjected to deparaffinization, rehydration, and antigen retrieval. Thereafter, the sections were labeled with PVRL4 and Ki67 antibodies overnight at 4°C and matched secondary antibodies at 37°C for 2 h. Following staining with diaminobenzidine (DAB) (Beyotime), the images were photographed and analyzed.

### 2.17 | Statistical Analysis

The data were manifested as the mean ± standard deviation (SD). Group comparison was conducted using the Student's t-test or analysis of variance followed by Tukey's post hoc test. $p < 0.05$ meant statistically significant.

## 3 | Results

### 3.1 | PVRL4 Is Highly Expressed in LUAD Tissues and Cells

According to the analysis based on the Ualcan, Gepia, and Timer databases, we found that PVRL4 was highly expressed in LUAD tissues (Figure 1A–C). Also, we confirmed that PVRL4 levels both at mRNA and protein levels were higher in clinical LUAD tissues compared with the normal tissues (Figure 1D–F). In addition, a high expression of PVRL4 in LUAD cell lines was observed relative to normal 16HBE cells (Figure 1G,H).

### 3.2 | PVRL4 Silencing Suppresses LUAD Cell Proliferation, Invasion, and Migration and Induces Cell Apoptosis

Next, the functions of PVRL4 on LUAD progression were studied. The sh-PVRL4 or sh-NC was designed and western blotting showed that sh-PVRL4 introduction in A549 and HCC827 cells markedly decreased PVRL4 expression relative to sh-NC (Figure 2A). Functionally, CCK-8 and colony formation assays suggested that PVRL4 silencing suppressed A549 and HCC827 cell proliferation (Figure 2B–D). Then, transwell and wound healing assays showed that the invasion and migration abilities of A549 and HCC827 cells were markedly impaired after PVRL4 knockdown (Figure 2E,F). Moreover, PVRL4 deficiency-induced apoptosis in A549 and HCC827 cells (Figure 2G).

### 3.3 | PVRL4 Silencing Impedes LUAD Growth In Vivo

Subsequently, we further investigated the role of PVRL4 on LUAD progression in vivo. As shown in Figure 3A,B, PVRL4 silencing suppressed LUAD growth, evidenced by smaller and lighter tumors. Then we found that levels of PVRL4 were decreased in xenograft tumors of sh-PVRL4 group (Figure 3C). IHC analysis also showed the PVRL4- or Ki67-positive cells in xenograft tumors of sh-PVRL4 group were decreased compared with sh-NC group (Figure 3D).

### 3.4 | PVRL4 Is Transferred Into PBMCs From LUAD Cells by Exosomes

Thereafter, we aimed to explore whether the oncogenic activity of PVRL4 has effects on the tumor microenvironment. The exosomes were isolated from A549 and HCC827 cells, named A549-Exo and HCC827-Exo. The extracellular A549-Exo and HCC827-Exo were identified by their typical cup-shaped morphology using TEM and by exosomal markers (CD9+, CD63+, and Alix+) (Figure 4A,B). Then isolated A549-Exo and HCC827-Exo were incubated with PBMCs. The uptake of A549-Exo and HCC827-Exo was observed using the PKH67 staining. We found that PKH67-labeled exosomes were localized in the cytoplasm, markedly endocytosed by PBMCs (Figure 4C). After incubation of A549-Exo and HCC827-Exo, levels of PVRL4 protein were increased in PBMCs (Figure 4D,E). In addition, PBMCs were also incubated with A549 or HCC827 cells, followed by GW4869 incubation. We discovered that PVRL4 protein levels were increased

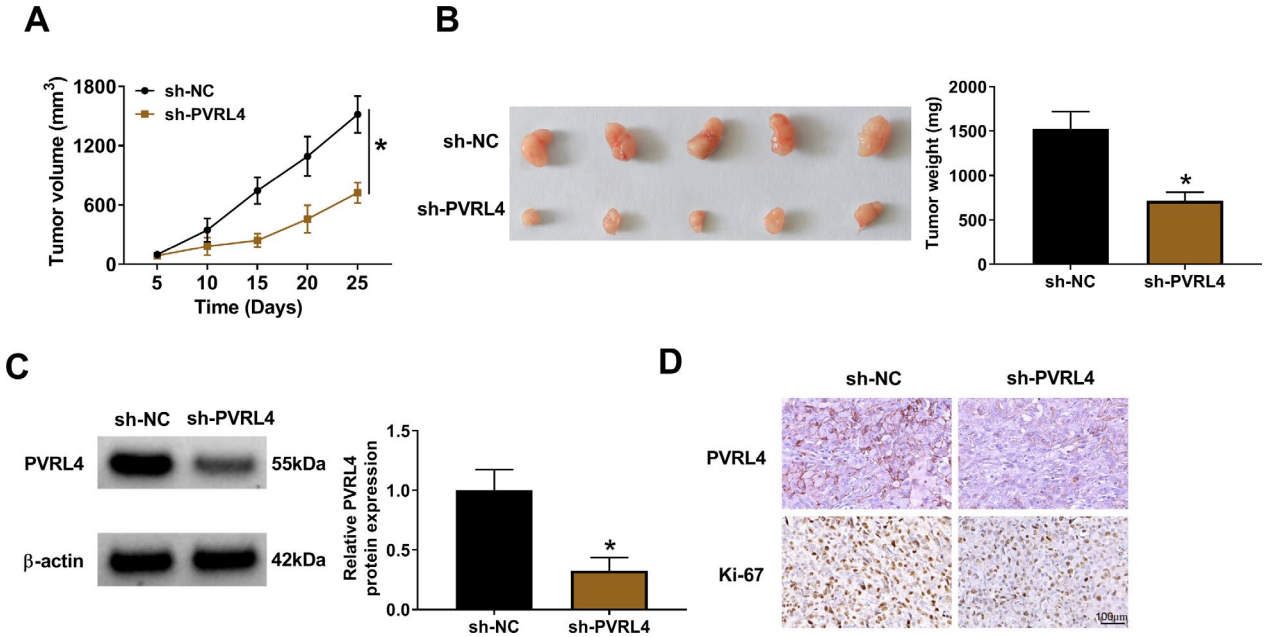


**FIGURE 3** | PVRL4 silencing impedes LUAD growth in vivo. (A, B) The growth curve of xenograft tumors. (B) Representative xenograft tumors and the weight of xenografts. (C) Western blotting for PVRL4 levels in xenograft tumors. (D) IHC analysis for Ki67 and PVRL4 in xenograft tumors. *$p < 0.05$.

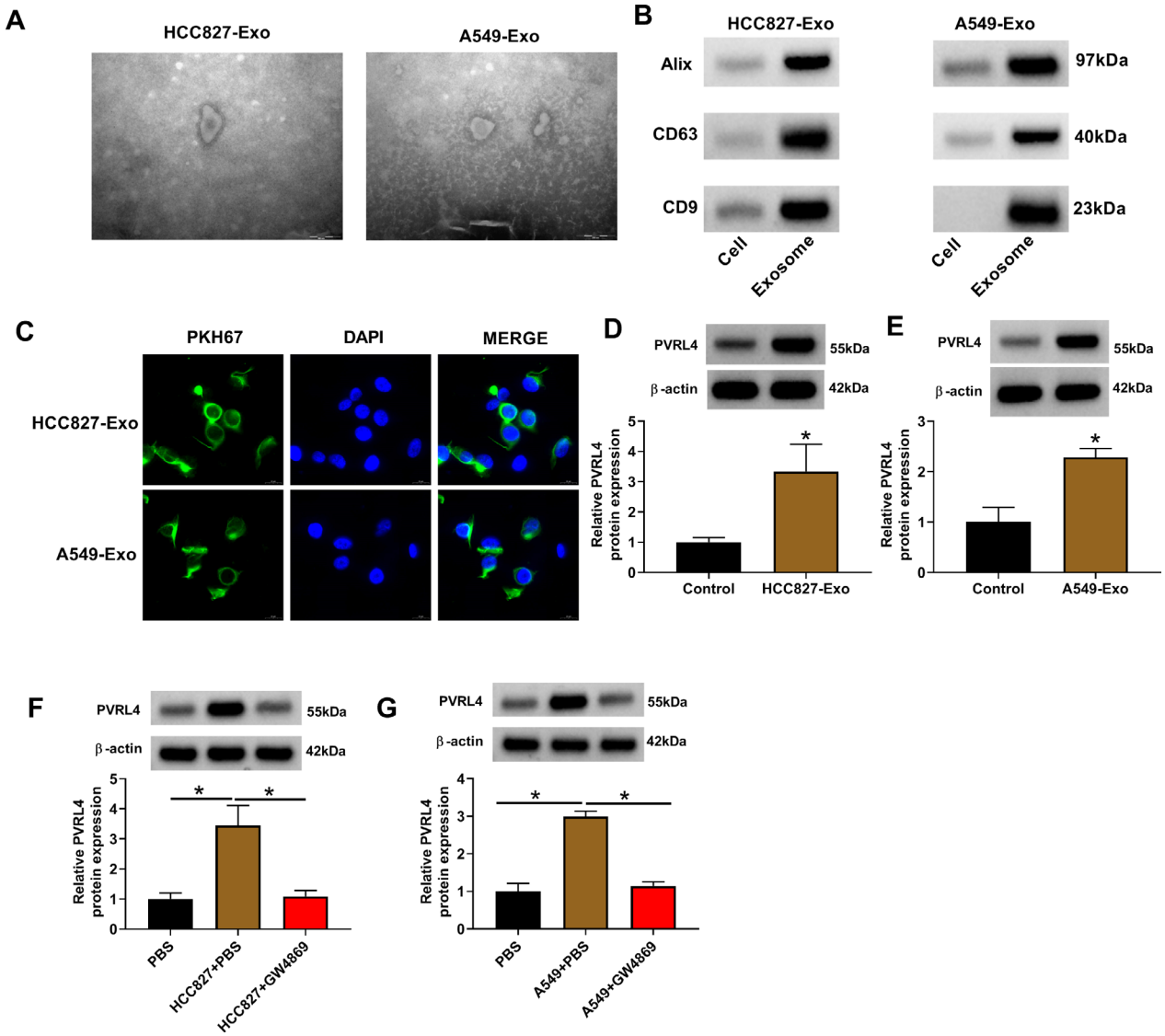


**FIGURE 4** | PVRL4 is transferred into PBMCs from LUAD cells by exosomes. (A) TEM analysis for exosome morphology. (B) Western blotting analysis for exosomal markers (CD9, CD63 and Alix). (C) The uptake of A549-Exo and HCC827-Exo was observed using the PKH67 staining. (D, E) Levels of PVRL4 protein were detected by western blotting in PMSCs after incubating with A549-Exo, HCC827-Exo or PBS (Control). (F, G) PBMCs were incubated with PBS, A549 or HCC827 cells and PBS, or A549 or HCC827 cells and GW4869, and levels of PVRL4 protein were examined by western blotting in PMSCs. $*p < 0.05$.

after A549 or HCC827 cell incubation, but decreased in the GW4869 incubation group (Figure 4F,G), further suggesting that PVRL4 could be transferred into PBMCs by LUAD cell exosomes.

### 3.5 | PVRL4 Knockdown in LUAD Cell-Exosomes Suppresses MDSC Induction and the Production of MDSC-Secreted TGF-β1

Next, the exosomes from A549 or HCC827 cells transfected with sh-MC or sh-PVRL4 were isolated, named HCC827-Exo$^{sh-NC}$, A549-Exo$^{sh-NC}$, HCC827-Exo$^{sh-PVRL4}$, or A549-Exo$^{sh-PVRL4}$, and incubated with PBMCs. Then, levels of PVRL4 were detected. Western blotting analysis showed that PVRL4 levels in PBMCs with HCC827-Exo$^{sh-PVRL4}$, or A549-Exo$^{sh-PVRL4}$ incubation were significantly decreased (Figure 5A). Flow cytometry suggested that the number of $CD14^{+}HLA\text{-}DR^{-}$ MDSCs was markedly decreased after HCC827-Exo$^{sh-PVRL4}$ or A549-Exo$^{sh-PVRL4}$ incubation, or PBS incubation compared with HCC827-Exo$^{sh-NC}$ or A549-Exo$^{sh-NC}$ incubation (Figure 5B,C), indicating that the decrease of exosomal PVRL4 led to the inhibition of MDSC induction. Moreover, ELISA and western blotting analyses suggested that levels of TGF-β1 that was secreted by MDSCs were decreased by HCC827-Exo$^{sh-PVRL4}$ or A549-Exo$^{sh-PVRL4}$ incubation (Figure 5D–G), suggesting that the deficiency of exosomal PVRL4 suppressed MDSC-secreted TGF-β1.

### 3.6 | Knockdown of Exosomal PVRL4 Suppresses LUAD Cell Proliferation, Invasion, and Migration and Induces Cell Apoptosis by Regulating MDSC-Secreted TGF-β1

To study whether exosomal PVRL4 affected LUAD by modulating MDSCs, we overexpressed TGF-β1 in MDSCs and incubated with LUAD cell lines that were pre-incubated with

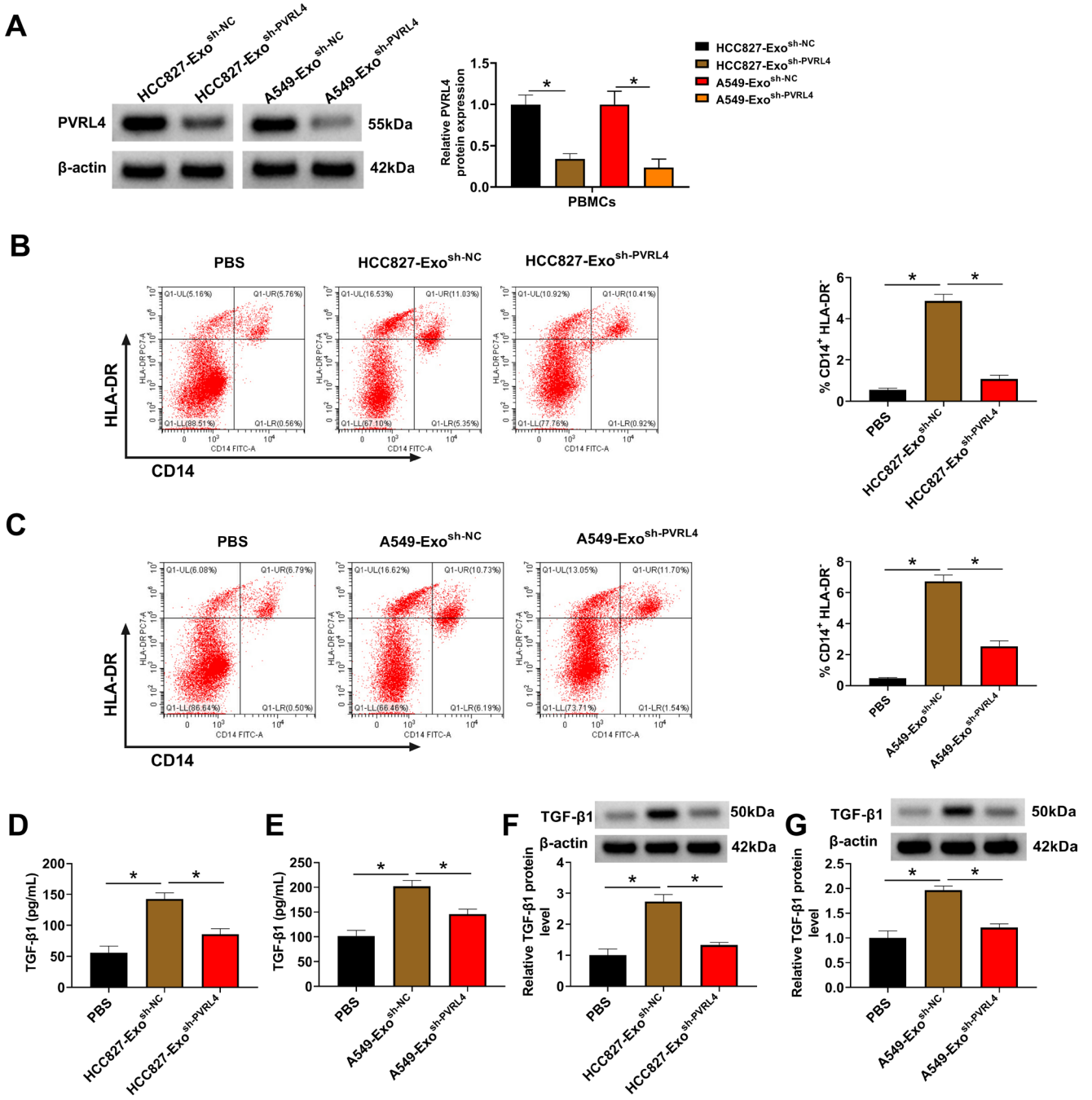


**FIGURE 5** | PVRL4 knockdown in LUAD cell exosomes suppresses MDSC induction and the level of MDSC-secreted TGF-β1. (A-G) PBMCs were incubated with PBS, HCC827-Exo$^{sh-NC}$, A549-Exo$^{sh-NC}$, HCC827-Exo$^{sh-PVRL4}$, or A549-Exo$^{sh-PVRL4}$. (A) Levels of PVRL4 were detected by western blotting. (B, C) Flow cytometry for the number of CD14$^{+}$HLA-DR$^{-}$ MDSCs after co-incubation. (D-G) ELISA analysis and western blotting for TGF-β1 levels in PBMCs after co-incubation. *$p < 0.05$.

HCC827-Exo$^{sh-NC}$, A549-Exo$^{sh-NC}$, HCC827-Exo$^{sh-PVRL4}$, or A549-Exo$^{sh-PVRL4}$. Western blotting analysis showed that levels of TGF-β1 were reduced by the knockdown of exosomal PVRL4 in LUAD cells despite under MDSC incubation and were then rescued by TGF-β1 overexpression in MDSCs (Figure 6A). Functionally, we found that the silencing of exosomal PVRL4 suppressed the proliferation (Figure 6B–E), invasion (Figure 6F,G), migration (Figure 6H,I), and induced the apoptosis (Figure 6J,K) in A549 and HCC827 cells, while these effects were counteracted by the incubation of TGF-β1 overexpressed MDSCs (Figure 6B–K).

## 4 | Discussion

In the present work, a highly expressed PVRL4 was observed in clinical LUAD tissues and cells, and was consistent with the database results. Functionally, PVRL4 silencing suppressed LUAD

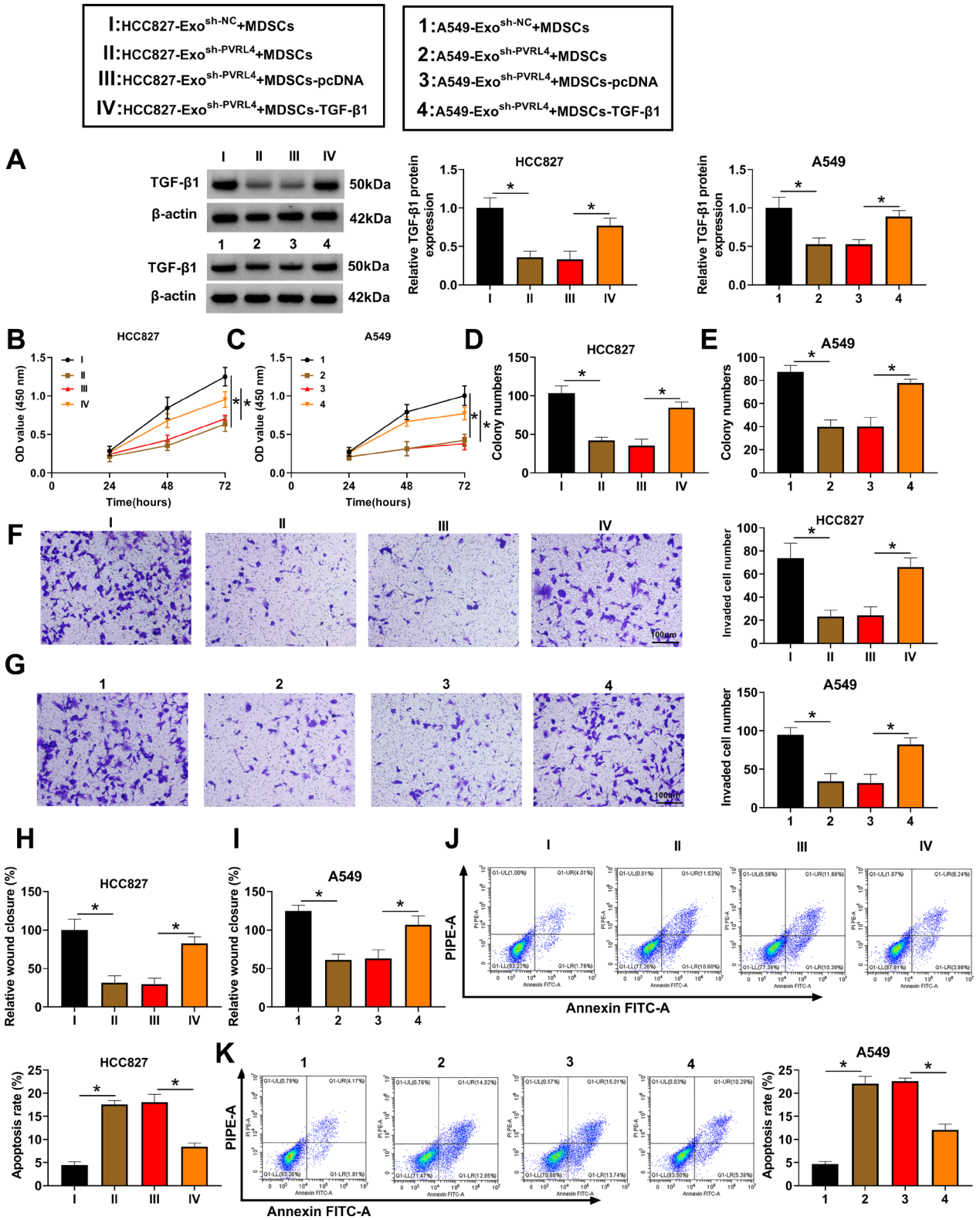


**FIGURE 6** | Knockdown of exosomal PVRL4 suppresses LUAD cell proliferation, invasion, and migration and induces cell apoptosis by regulating MDSC-secreted TGF-β1. (A-K) A549 and HCC827 cells were incubated with TGF-β1 overexpressed MDSCs, followed by incubating with HCC827-Exo$^{sh-NC}$, A549-Exo$^{sh-NC}$, HCC827-Exo$^{sh-PVRL4}$, or A549-Exo$^{sh-PVRL4}$. (A) Levels of PVRL4 were detected by western blotting. (B–E) CCK-8 and colony formation assays for cell proliferation. (F, G) Transwell for cell invasion. (H, I) Wound healing assay for cell migration. (J, K) Flow cytometry analysis for cell apoptosis. *$p < 0.05$.

cell proliferation, invasion, migration and induced cell apoptosis. Further in vivo assay also suggested that the deficiency of PVRL4 hampered LUAD growth in mouse models. This data validated the oncogenic roles of PVRL4 in LUAD progression. Till date, PVRL4 has long been a potential therapeutic target of interest to researchers due to its endocytotic characteristics [20].

Fujiyuki et al. established a recombinant measles virus to infect host cells by binding to PVRL4 for oncolytic virus therapy, and was demonstrated to impede xenograft growth in breast and pancreatic cancers [21, 22]. The first enfortumab vedotin antibody-drug conjugate targeting PVRL4 (AGS-22M6) have been approved by the FDA for urothelial carcinoma treatment, which induces cell apoptosis by destroying microtubules via monomethyl auristatin E release [23, 24]. Thus, it is conceivable to foster that PVRL4 siRNAs or shRNAs may be promising agents for LUAD therapy.

Nevertheless, the low response rate because of endothelial barrier and the emergence of drug resistance have been identified to limit the potency of molecular targeted therapy [7, 12]. Exosomes, secreted by most cells, are one kind of nano-sized small extracellular vesicles ranging from 30 to 150 nm in diameter. They can transmit signals and molecules, such as nucleic acids, lipids, proteins, glycoconjugates, and other bioactive substances, to local or distant recipient cells, thereby impacting cellular physiological and pathological processes [25–27]. Moreover, exosomes have been identified to be high physicochemical stability, well tolerated, and low immunogenicity, as well as possess the ability to cross the blood brain barrier; therefore, they are ideal drug delivery carriers for cell-free therapy [28, 29]. Herein, we conformed that PVRL4 was packaged into exosomes in LUAC cells and could be transfer into other cells via exosomes, further exhibiting the feasibility of therapeutic strategy to target and inhibit PVRL4 activity in LUAD. Importantly, we found that the knockdown of exosomal PVRL4 markedly suppressed LUAD cell proliferation, invasion, migration and induced cell apoptosis by down-regulating MDSC-secreted TGF-β1. MDSCs are heterogeneous, immature cell populations of myeloid origin that promote tumor immune escape and protect tumor cells against the host immune system attack in the tumor microenvironment (TEM) [30, 31]. There is compelling evidence that MDSCs are major inhibitors of the anticancer response, they accelerate cancer growth by inducing the production of immunosuppressive molecules in the TME, such as TGF-β, IL-10, and reactive oxygen species, suppressing T cell activation via expressing cell surface receptors, or enhancing cell growth and invasion through producing matrix metalloproteinases and vascular endothelial growth factor [32, 33]. Collectively, it is conceivable to impair MDSCs as a viable therapeutic method for improving the efficacy of anti-tumor immunotherapy, since emerging evidence has confirmed the significant role of MDSCs in cancer mouse models and cancer patients, and their roles were implicated in enhancing MDSC differentiation, reducing MDSC accumulation and expansion, preventing the migration of MDSCs to tumor sites or the production of immunosuppressive molecules [34–36]. In the present work, we proved that PVRL4 knockdown in LUAD cell-exosomes suppressed MDSC accumulation and the production of MDSC-secreted TGF-β1, further indicating the oncogenic activity of PVRL4 on LUAD.

In conclusion, knockdown of exosomal PVRL4 suppressed LUAD progression by reducing MDSC induction and TGF-β1 production, which provide new insights into the development of potential molecular targets for the treatment of LUAD from a clinical perspective.

### Author Contributions

Study concept and design: Yahai Liang. Analysis and interpretation of data: Jinmei Li, Lihua Zhang, Jinling Zhou, Meilian Liu, Xiaoxia Peng, Weizhen Zheng. Drafting of the manuscript: Yahai Liang. Critical revision of the manuscript for important intellectual content: Zhennan Lai. Statistical analysis: Yahai Liang and Zhennan Lai. Study supervision: Yahai Liang and Jinmei Li.


### Acknowledgments

The authors have nothing to report.


### Conflicts of Interest

The authors declare no conflicts of interest.

### Data Availability Statement

Data sharing is not applicable to this article as no datasets were generated or analyzed during the current study.

### References


1. D. J. Myers and J. M. Wallen, "Lung Adenocarcinoma," in *StatPearls* (Treasure Island, FL: StatPearls Publishing, 2023).

2. Z. Guo, J. Liang, X. Zhang, et al., "PCM1: A Potential Prognostic Biomarker Correlated With Immune Infiltration in Lung Adenocarcinoma," *Current Proteomics* 20 (2023): 208–221.

3. C. C. Hao, C. Y. Xu, X. Y. Zhao, et al., "Up-Regulation of VANGL1 by IGF2BPs and miR-29b-3p Attenuates the Detrimental Effect of Irradiation on Lung Adenocarcinoma," *Journal of Experimental & Clinical Cancer Research* 39 (2020): 256.

4. Z. Wang, J. Zhang, S. Shi, et al., "Predicting Lung Adenocarcinoma Prognosis, Immune Escape, and Pharmacomic Profile From Arginine and Proline-Related Genes," *Scientific Reports* 13 (2023): 15198.

5. C. Zhou, Z. Jing, W. Liu, Z. Ma, S. Liu, and Y. Fang, "Prognosis of Recurrence After Complete Resection in Early-Stage Lung Adenocarcinoma Based on Molecular Alterations: A Systematic Review and meta-Analysis," *Scientific Reports* 13 (2023): 18710.

6. L. Zhong, Y. Li, L. Xiong, et al., "Small Molecules in Targeted cancer Therapy: Advances, Challenges, and Future Perspectives," *Signal Transduction and Targeted Therapy* 6 (2021): 201.

7. Y. T. Lee, Y. J. Tan, and C. E. Oon, "Molecular Targeted Therapy: Treating cancer With Specificity," *European Journal of Pharmacology* 834 (2018): 188–196.

8. X. Ke and L. Shen, "Molecular Targeted Therapy of cancer: The Progress and Future Prospect," *Frontiers in Laboratory Medicine* 1 (2017): 69–75.

9. J. Y. Li, Y. P. Chen, Y. Q. Li, N. Liu, and J. Ma, "Chemotherapeutic and Targeted Agents Can Modulate the Tumor Microenvironment and Increase the Efficacy of Immune Checkpoint Blockades," *Molecular Cancer* 20 (2021): 27.

10. D. G. Savage and K. H. Antman, "Imatinib Mesylate – A New Oral Targeted Therapy," *New England Journal of Medicine* 346 (2002): 683–693.

11. H. Y. Min and H. Y. Lee, "Molecular Targeted Therapy for Anticancer Treatment," *Experimental & Molecular Medicine* 54 (2022): 1670–1694.

12. D. M. K. Keefe and E. H. Bateman, "Potential Successes and Challenges of Targeted Cancer Therapies," *Journal of the National Cancer Institute. Monographs* 2019, no. 53 (2019): lgz008.

13. E. Shtivelman, T. Hensing, G. R. Simon, et al., "Molecular Pathways and Therapeutic Targets in Lung cancer," *Oncotarget* 5 (2014): 1392–1433.

14. N. Reymond, S. Fabre, E. Lecocq, J. Adelaide, P. Dubreuil, and M. Lopez, "Nectin4/PRR4, a New Afadin-Associated Member of the Nectin Family That Trans-Interacts With nectin1/PRR1 Through V Domain Interaction," *Journal of Biological Chemistry* 276 (2001): 43205–43215.

15. J. Zeindler, S. D. Soysal, S. Piscuoglio, et al., "Nectin-4 Expression Is an Independent Prognostic Biomarker and Associated With Better Survival in Triple-Negative Breast Cancer," *Frontiers in Medicine* 6 (2019): 200.

16. K. L. Boylan, P. C. Buchanan, R. D. Manion, et al., "The Expression of Nectin-4 on the Surface of Ovarian cancer Cells Alters Their Ability to Adhere, Migrate, Aggregate, and Proliferate," *Oncotarget* 8 (2017): 9717–9738.

17. J. Kobecki, P. Gajdzis, G. Mazur, and M. Chabowski, "Nectins and Nectin-Like Molecules in Colorectal Cancer: Role in Diagnostics, Prognostic Values, and Emerging Treatment Options: A Literature Review," *Diagnostics (Basel, Switzerland)* 12, no. 12 (2022): 3076.

18. S. Chatterjee, S. Sinha, and C. N. Kundu, "Nectin Cell Adhesion Molecule-4 (NECTIN-4): A Potential Target for cancer Therapy," *European Journal of Pharmacology* 911 (2021): 174516.

19. K. Tamura, K. Ishigaki, O. Yoshida, et al., "Gene Expression of Nectin-4 and Its Clinical Significance in Dogs With Primary Lung Adenocarcinoma," *Veterinary Medicine and Science* 8 (2022): 1922–1929.

20. M. Hammood, A. W. Craig, and J. V. Leyton, "Impact of Endocytosis Mechanisms for the Receptors Targeted by the Currently Approved Antibody-Drug Conjugates (ADCs)-A Necessity for Future ADC Research and Development," *Pharmaceuticals (Basel)* 14 (2021): 674.

21. T. Fujiyuki, Y. Amagai, K. Shoji, et al., "Recombinant SLAMblind Measles Virus Is a Promising Candidate for Nectin-4-Positive Triple Negative Breast Cancer Therapy," *Molecular Therapy - Oncolytics* 19 (2020): 127–135.

22. M. Awano, T. Fujiyuki, K. Shoji, et al., "Measles Virus Selectively Blind to Signaling Lymphocyte Activity Molecule Has Oncolytic Efficacy Against Nectin-4-Expressing Pancreatic cancer Cells," *Cancer Science* 107 (2016): 1647–1652.

23. P. M. Challita-Eid, D. Satpayev, P. Yang, et al., "Enfortumab Vedotin Antibody-Drug Conjugate Targeting Nectin-4 Is a Highly Potent Therapeutic Agent in Multiple Preclinical Cancer Models," *Cancer Research* 76 (2016): 3003–3013.

24. E. I. Heath and J. E. Rosenberg, "The Biology and Rationale of Targeting Nectin-4 in Urothelial Carcinoma," *Nature Reviews. Urology* 18 (2021): 93–103.

25. J. Shao, J. Zaro, and Y. Shen, "Advances in Exosome-Based Drug Delivery and Tumor Targeting: From Tissue Distribution to Intracellular Fate," *International Journal of Nanomedicine* 15 (2020): 9355–9371.

26. C. He, S. Zheng, Y. Luo, and B. Wang, "Exosome Theranostics: Biology and Translational Medicine," *Theranostics* 8 (2018): 237–255.

27. A. K. Ludwig and B. Giebel, "Exosomes: Small Vesicles Participating in Intercellular Communication," *International Journal of Biochemistry & Cell Biology* 44 (2012): 11–15.

28. S. Sadeghi, F. R. Tehrani, S. Tahmasebi, A. Shafiee, and S. M. Hashemi, "Exosome Engineering in Cell Therapy and Drug Delivery," *Inflammopharmacology* 31 (2023): 145–169.

29. Y. Yang, Y. Ye, X. Su, J. He, W. Bai, and X. He, "MSCs-Derived Exosomes and Neuroinflammation, Neurogenesis and Therapy of Traumatic Brain Injury," *Frontiers in Cellular Neuroscience* 11 (2017): 55.

30. D. I. Gabrilovich, "Myeloid-Derived Suppressor Cells," *Cancer Immunologic Research* 5 (2017): 3–8.

31. J. E. Talmadge and D. I. Gabrilovich, "History of Myeloid-Derived Suppressor Cells," *Nature Reviews. Cancer* 13 (2013): 739–752.

32. H. Hu, Y. Xiang, T. Li, et al., "Induction of M-MDSCs With IL6/GM-CSF From Adherence Monocytes and Inhibition by WP1066," *Experimental and Therapeutic Medicine* 24 (2022): 487.

33. X. Gao, H. Sui, S. Zhao, X. Gao, Y. Su, and P. Qu, "Immunotherapy Targeting Myeloid-Derived Suppressor Cells (MDSCs) in Tumor Microenvironment," *Frontiers in Immunology* 11 (2020): 585214.

34. F. M. Consonni, C. Porta, A. Marino, et al., "Myeloid-Derived Suppressor Cells: Ductile Targets in Disease," *Frontiers in Immunology* 10 (2019): 949.

35. A. M. K. Law, F. Valdes-Mora, and D. Gallego-Ortega, "Myeloid-Derived Suppressor Cells as a Therapeutic Target for Cancer," *Cells* 9 (2020): 9.

36. A. Salminen, A. Kauppinen, and K. Kaarniranta, "AMPK Activation Inhibits the Functions of Myeloid-Derived Suppressor Cells (MDSC): Impact on cancer and Aging," *Journal of Molecular Medicine (Berlin, Germany)* 97 (2019): 1049–1064.